

## Overview of recent developments in organic thin-film transistor sensor technology

M. C. TANESE, F. MARINELLI, D. ANGIONE and L. TORSI

*Dipartimento di Chimica, Università di Bari - Via Orabona 4, 70126 Bari, Italy*

(ricevuto il 7 Gennaio 2009; approvato il 18 Febbraio 2009; pubblicato online il 23 Marzo 2009)

**Summary.** — Bio and chemical sensing represents one of the most attractive applications of organic electronics and of Organic Thin Film Transistors (OTFTs) in particular. The implementation of miniaturized portable systems for the detection of chemical analytes as well as of biological species, is still a challenge for the sensors' community. In this respect OTFTs appear as a new class of sensors able, in principle, to overcome some of the commercial sensors drawbacks. As far as volatile analytes are concerned, commercially available sensing systems, such as metal oxide based chemi-resistors, offer great stability but rather poor selectivity. In spite of the improved selectivity offered by organic chemi-resistors the reliability of such devices is not yet satisfactorily proven. On the other hand, complex odors recognition, but also explosives or pathogen bacteria detection are currently being addressed by sensor array systems, called "e-noses", that try to mimic the mammalian olfactory system. Even though potentially very effective, this technology has not yet reached the performance level required by the market mostly because miniaturization and cost effective production issues. OTFT sensors can offer the advantage of room temperature operation and deliver high repeatable responses. Beside, they show very good selectivity properties. In fact, they implement organic active layers, which behave as sensing layers as well. This improves OTFTs sensitivity towards different chemical and biological analytes as organic materials can be properly chemically tailored to achieve differential detection and potentially even discrimination of biological species. In addition to this, OTFTs are also able to offer the unique advantages of a multi-parametric response and a gate bias enhanced sensitivity. Recently thin dielectric low-voltage OTFTs have also been demonstrated. Their implementation in low power consumption devices has attracted the attention of the organic electronic community. But such low power transistors have also a great potential in sensing applications specifically those performed in a liquid environment. In fact, low-voltage OTFTs have been recently demonstrated to deliver reliable responses even when operated in water for hundreds of measurement cycles. This opens new perspectives in the field of cheap, low-power and mass-produced aqueous sensors.

PACS 81.07.Bc – Nanocrystalline materials.

PACS 82.35.Cd – Conducting polymers.

PACS 85.30.Tv – Field effect devices.

PACS 87.85.fk – Biosensors.

## 1. – Introduction

The field of OTFT sensors has attracted great attention in the last decade. This is mainly due to the possibility to implement such devices in high performances portable sensing systems. One of the major sensor market's requirements is for devices capable of on-line and *in situ* detection of chemical and biological analytes for a broad variety of applications that ranges from food and beverage control to medical diagnostic and public security. These needs are presently not yet satisfactorily fulfilled by commercial sensor technology. Selectivity, room temperature operation and high sensitivity to a broad range of analytes are still open issues for the available technologies and in this respect OTFTs hold the potential to overcome some of their drawbacks. Indeed they behave as multi-parameter sensors, show very high repeatable, fast and reversible responses [1], allow for room temperature operation, offer good selectivity towards a broad range of analytes [2], and enable sensing switch showing a gate enhanced sensitivity [3]. They can also be operated in the subvoltage regime resulting in very low power consumption devices [4-6].

Current sensing instruments are mostly based on two technologies: metal-oxide resistive sensors, and inorganic field-effect sensors. Metal-oxide based chemi-resistors are two-terminal devices employing gas-sensitive metal-oxide active layers such as SnO<sub>2</sub> and ZnO [7-10]. In such devices, the gas analyte is detected by means of a single parameter response, namely the change in the metal-oxide semiconductor active layer bulk resistivity. Even though chemi-resistors responses are highly stable and show good sensitivity, these sensors are not very selective. In addition to this they require high operation temperatures to achieve fully desorption of chemisorbed analyte molecules. Chemi-resistor selectivity can be improved by implementing organic active layers instead of metal-oxide films [7, 11] showing anyhow poor reliability due to sensitivity to humidity and long-term drift.

Inorganic field-effect gas sensors, on the other hand, have found their main application as high sensitivity hydrogen sensors. They are also known as chemically sensitive field-effect transistors (CHEMFETs). Their structure is that of a silicon-based MOSFET top gate transistors whose sensing element is constituted by the gate electrode material. The electrical transport is here confined in the semiconductor region which is never in contact with the analyte [9, 12-17] while the transduction is given by the variation of the transistor threshold voltage,  $V_t$  [16]. As for chemi-resistors also CHEMFETs are single parameter sensors. Implementation of CPs gate materials helps in broadening CHEMFET selectivity [14] with the advantage of detecting  $V_t$  changes by passing a very low current through the conducting polymer. This makes CHEMFETs generally more stable than chemi-resistors. However, detected concentrations are still in the high parts per million range, and responses are fairly reversible, although a systematic study has never been published.

OTFTs are quite different devices compared to the elicited two classes of sensors. A schematic representation of a sensing OTFT is given in fig. 1. They are bottom gate field effect transistors employing polycrystalline organic active layers acting at the same time as sensing membrane when the OTFT is exposed to the analyte to be revealed. The organic layer/analyte interaction can be detected by monitoring the variation of the current flowing in the OTFT while operated in its two characteristic modes, which will be described in the following. OTFT exposure to chemical analytes generally results in fast, room temperature and reversible responses towards a wide range of organic molecules [2]. The three-terminal structure of OTFTs happens to be advantageous

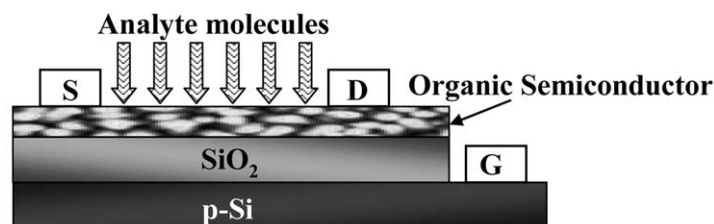


Fig. 1. – Schematic overview of an OTFT sensor.

allowing for multi-parametric responses eventually increasing the analyte detection capabilities. Recently Grell's group has developed a system for simultaneous extraction of OTFT figures of merits [5]. It has also been demonstrated that by playing with the voltages applied to the three OTFT electrodes, source drain and gate, it is possible to obtain a response enhancement for different sensor/analyte systems at fixed concentrations [3, 17]. OTFT structure also allows to obtain full recovery of pristine operation conditions without the need of high temperatures since they can be reset by a proper biasing of the gate after each measurement. OTFT responses are therefore highly repeatable showing a recovery of the signal within the 2% over several tens of repeated exposure cycles [2]. As far as selectivity is concerned it has been demonstrated that it is possible to modulate OTFT selectivity by proper chemical tuning of the organic active layers with *ad hoc* chosen chemical substituents [17].

In the present review the OTFT operation as well as their sensing properties will be discussed. Particularly it will be shown how it is possible to achieve substantial selectivity improvement by exploiting the properties of the chemical substituents attached to the OTFTs organic semiconductors backbones. OTFT sensing switch properties will be examined as well. Finally recent advances in low-operation voltages OTFTs for in liquid biological tests will be also reported.

## 2. – OTFT structure and operation

OTFTs are three-terminal field-effect transistors in which the current flowing between the two source and drain terminals is controlled by modulating the electrical potential of the third terminal, namely the gate electrode. Figure 2 shows the two possible OTFT

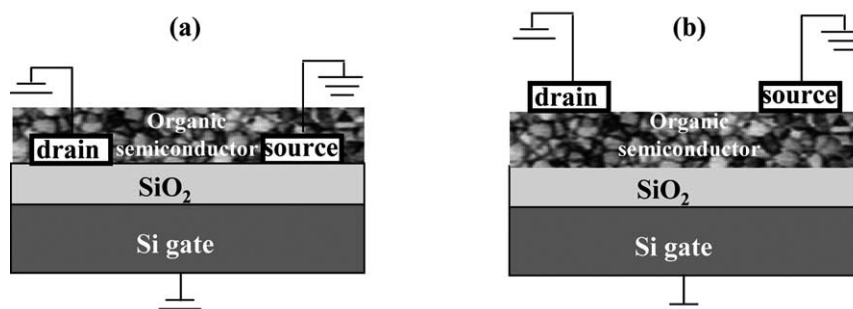


Fig. 2. – Basic structure of bottom contact (a) and top contact (b) OTFT devices.

geometries, namely the top and bottom contact ones. Both configurations consist of a highly doped silicon substrate covered by a thin dielectric film that is interfaced to the organic active layer. In the case of bottom contact devices, gold source and drain contacts are defined by means of photolithographic techniques directly on the dielectric layer and they are topped with the organic semiconductor thin film acting as conducting material. In top contact OTFTs, on the contrary, source and drain electrodes are defined by gold thermal evaporation through a shadow-mask over the organic active layer. Both structures are bottom gate transistors with the gate contact taken directly on the silicon substrate. As shown in fig. 2, OTFTs are operated in the common source configuration, connecting the source contact to ground and biasing the gate and the drain contacts against it. The gate bias,  $V_g$ , controls the current,  $I_d$ , flowing into the organic active layer between source and drain electrodes under an imposed bias,  $V_d$ . Plastic substrates, polymeric insulators and conductive inks for source and drain electrodes definition are also being developed for flexible electronics applications.

The bottom-contact structure is commonly used in the field of organic electronics to characterize new materials as their fabrication procedure is quite an easy one. The whole structure except for the active layer can be built and patterned using standard photolithography and micro-fabrication techniques. However, depositing organic materials on a substrate with predefined source and drain contacts generally causes poor morphological/structural organization of the organic semiconductor at the contacts interfaces. In fact, surface energy and surface roughness differences between electrodes and dielectric can originate different organic semiconductor microstructures, resulting in disordered regions at the source/drain contacts. Hence, bottom-contact structures typically suffer from larger source and drain contact barriers and contact resistances [18,19].

Top contact structures are characterized, on the contrary, by better ordered organic thin films but they have channel dimensions limited by the shadow mask features that cannot be much lower than 50 micrometers. Top contact, metal evaporated OTFT technology is however not suitable for large-scale manufacturing, nevertheless such geometry allows for a more effective charge injection into the organic semiconductor, higher mobilities and lower contact resistance due to the better contact between the semiconductor and the electrodes.

OTFT active materials, where the conduction takes place, are generally made of conjugated polymers or oligomers, such as regioregular polythiophenes or pentacene molecules, deposited as films, few tens of nanometers thick. Film formation is achieved by means of different deposition techniques such as solution casting, spin coating, and Langmuir-Shäfer or Langmuir-Blodgett techniques for solution processed thin film and thermal evaporation for molecules with low degree of solubility. Figures 3 (a) and (b) show the chemical structure of some p- and n-type organic semiconductors used as active layer in OTFTs [20].

All these organic materials usually result in polycrystalline thin films exhibiting a granular morphology consisting of grains having a crystalline-type degree of structural order with linear dimensions generally of about hundreds of nanometers.

In the following the operation of an OTFT will be explained considering the case of a p-type channel material-OTFT as benchmark configuration. Two gold pads, having a width  $W$  (channel width) and separated by a distance  $L$  (channel length), constitute the OTFT source and drain electrodes. It is to be pointed out that gold is chosen for source and drain definition because its work function is similar to the energy of the HOMO of most p-type organic semiconductors and should lead in principle to the formation of ohmic contacts. As mentioned before, the drain and the gate voltages,  $V_d$

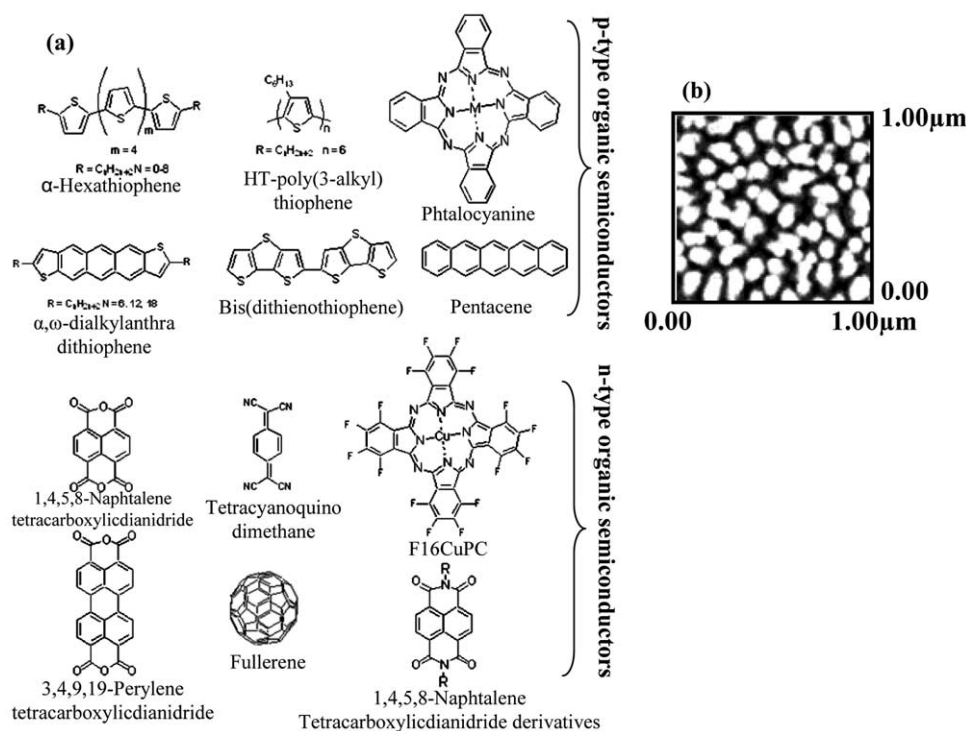


Fig. 3. – Chemical structures of different p- and n-type organic semiconductors (a) employed as OTFT active layers [20]; (b) AFM image of a pentacene thin film deposited by thermal evaporation.

and  $V_g$ , are usually taken with respect to the source electrode which is grounded. The gate bias ( $V_g$ ) controls the flux of carrier current,  $I_d$ , flowing between source and drain electrodes under an imposed bias  $V_d$ . When a negative voltage is applied to the gate electrode, a hole transport takes place. Similarly, by applying a positive voltage to the gate electrode electron transport is obtained in the case of n-channel devices. In order to better understand the OTFT operation it is here considered the cross-sectional view of an OTFT energy band structure along the metal-insulator-organic semiconductor junction for different gate voltages (fig. 4).

The energy-band diagram of fig. 4 is here given for a p-type organic semiconductors (similar diagrams can be produced for n-type materials). The bands edges are referred to the vacuum level ( $V_L$ ) and the material electrochemical potentials (or equivalently the Fermi levels,  $E_F$ ) are reported. The positive charges are hole-type polaronic carriers [21-23] generated by the doping effect of adventitious impurities but also of film structural irregularities [24-26]. These are uniformly distributed in the film. By applying a negative  $V_d$  bias, a low current of positive charge will be observed. This is called *off*-current and is proportional to the organic thin film bulk (or 3D-type) conductivity. In other words, the device is in the *off*-state. When a negative voltage is applied to the gate contact, as shown in fig. 4 a), the organic semiconductor bands will bend upwards and the energy of the HOMO level will move closer to the Fermi level producing an accumulation of positive charge carriers (holes) at the semiconductor-insulator interface.

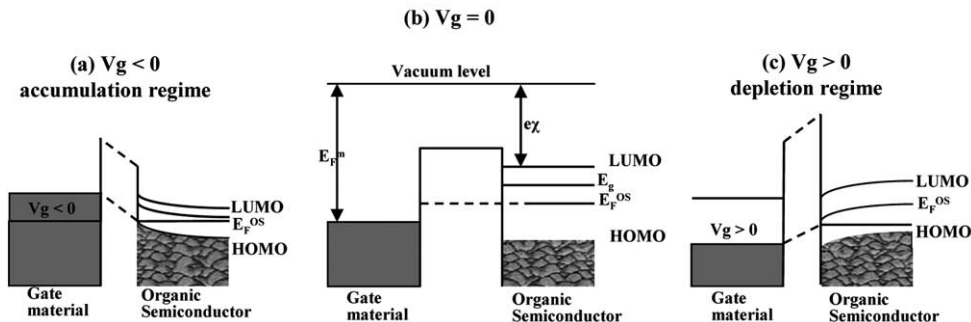


Fig. 4. – Band diagram of the MIS junction for the three conducting regimes of a TFT for a p-type semiconductor: accumulation (a), off (b), depletion (c) regimes.

By biasing the device with a negative voltage  $V_d$  a holes current will flow in the channel region. In this regime, the OTFT operates in the enhancement mode and it is said to be in the *on*-state. This field-induced conductivity has been shown to be two dimensional, as no conductivity increase was measured upon increase of the active material thickness by two orders of magnitude [27].

On the contrary, when a positive voltage is applied to the gate electrode, the opposite band bending occurs causing a depletion of majority carriers (holes) at the semiconductor-insulator interface as shown in fig. 4c). Most probably due to the presence of traps in the organic active layer and to the high energy barrier for electron injection at the metal-semiconductor contacts a polycrystalline OTFT generally cannot work in inversion regime. Hence, in contrast to the Si MOSFETs where an inversion regime is reached [28] with increasing the gate voltage, a (p-type) OTFT always operates in accumulation mode and the current is made up of majority charge carriers. Summarizing, two distinct regimes of charge conduction can take place in an OTFT device. When no voltage is applied to the gate electrode (*off*-state) a bulk conduction occurs involving intrinsic organic thin-film charge carrier due to unintentional doping. This is clearly a bulk effect. On the contrary when a negative gate voltage (beyond threshold) is applied, charge carriers are induced in the organic semiconductor at the interface with the gate dielectric. The charges induced in this region increases by increasing the gate bias applied and this generates a gate modulated *on*-state.

Two different OTFT current-voltage ( $I$ - $V$ ) outputs can be measured by biasing gate and source/drain electrodes: the  $I_d$ - $V_d$  characteristics and the  $I_d$ - $V_g$  transfer characteristics curves. The  $I_d$ - $V_d$  output characteristic curves represent the  $I_d$  current as a function of the  $V_d$  voltage at fixed  $V_g$ . By changing the  $V_g$  bias at each single  $V_d$  sweep a family of  $I$ - $V$  characteristics curves is obtained. It clearly appears, analyzing these curves, that the higher the gate voltage applied, the larger the current flowing in the channel region. The transfer characteristic curves, on the other hand, are generally displayed by a plot of the drain current,  $I_d$ , as a function of the gate voltage,  $V_g$ , at a fixed source-drain  $V_d$  bias. A transfer characteristics curve shows how effectively the gate voltage can switch the device from the *off* to the *on* state.

An example of the  $I_d$ - $V_d$  characteristics curves and  $I_d$ - $V_g$  transfer-characteristics plot of a representative OTFT is given in fig. 5 a) and b).

OTFT  $I_d$ - $V_d$  curves look very similar to those of inorganic FETs [28,29]. Indeed they show linear and saturation  $I_d$  current regions occurring at  $V_d$  biases much lower or higher

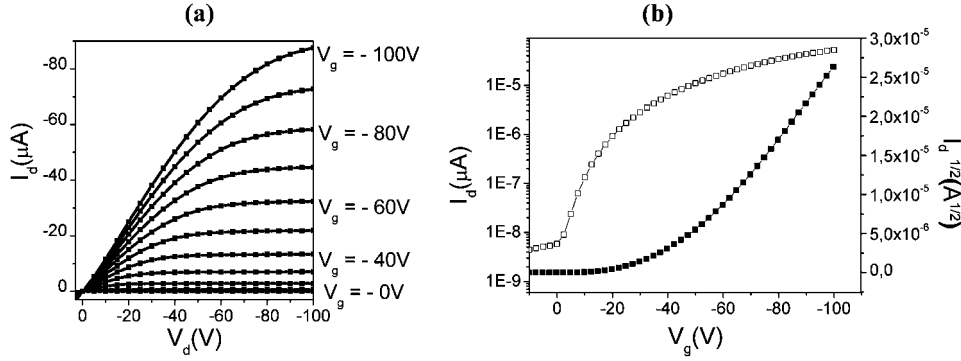


Fig. 5. – Typical  $I_d$ - $V_d$  current-voltage characteristics (a) and  $I_d$ - $V_g$  transfer-characteristics curve of a thiophene based OTFT.

than  $(V_g - V_t)$  respectively,  $V_t$  being the transistor threshold voltage. In other words, the  $I_d$  current linearly increases with the source-drain voltage until the channel is pinched-off and the current tends to a saturation value.

The analytical equations for the description of the OTFT  $I_d$ - $V_d$  curves, taken directly from those used for standard inorganic FET [28, 30] are reported below:

$$(1) \quad I_d = \frac{W}{L} \mu C_i \left( V_g - V_t - \frac{V_d}{2} \right) V_d, \quad V_d \ll (V_g - V_t),$$

$$(2) \quad I_{d,\text{sat}} = \frac{W}{2L} \mu C_i (V_g - V_t)^2, \quad V_d > (V_g - V_t),$$

$$(3) \quad V_t^{\text{TFT}} = \frac{qNd}{C_i}.$$

Here  $C_i$  is the OTFT capacitance per unit area while  $\mu$  is the field-effect mobility. The current in the linear regime is expressed by eq. (1), while the quadratic function of the gate voltage-current is clearly observed in eq. (2). OTFTs figures of merit are the field-effect mobility ( $\mu$ ), the threshold voltage ( $V_t$ ) and the *on-off* ratio ( $I_{\text{on}}/I_{\text{off}}$ ). It is to be pointed out that although the standard MOSFET equations allow for a good estimate of the OTFT figures of merit they do not fully and properly describe the OTFT behavior. In fact, OTFTs suffer from significant non-idealities at the contacts. This can be addressed by considering contact resistance and contact injection barriers. Even though such correction improves the accuracy of the model, it does not take into account other aspects, such as the gate-bias-dependent mobility, the thermally activated transport, and the gradual turn-on of characteristics, that cannot be explained by a direct translation of the bulk silicon MOSFET theory to the OTFT devices.

### 3. – OTFT sensing properties

OTFT operation makes this class of devices very attractive in sensing application mainly because they can be used as multi-parameter sensors [1]. As previously discussed they can be operated in the *off* and *on* modes. For this reason they are able to deliver two distinct sets of responses, one recorded in the *off* state, the other in the *on* state.

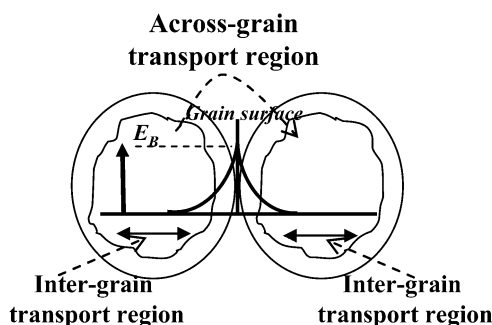


Fig. 6. – Schematic diagram of the potential barriers at grain boundaries of the OTFT sensing layer.

When the OTFT is in the *off* state OTFT it essentially behaves as a chemi-resistors. Here the OTFT current is dominated by the intrinsic bulk charge carriers of the organic semiconductor film. On the other hand, an above threshold gate voltage switches *on* the OTFT. If exposed to a chemical analyte while in its *on* state, all OTFT figures of merit are influenced, undergoing eventually a change. The OTFT current changes in the *on*- and *off*-states can be different. Indeed, while the chemically induced parameter variations taking place in the *off* state only depend on the organic material bulk properties, the *on* state responses, on the contrary, can be gate bias depending. The charge density in the channel is increased by increasing the gate bias applied, resulting in a gate-dependent density of charges available for possible interaction with an analyte. The higher the gate bias applied, the higher the density of charges in the channel and the higher the OTFT response at a fixed analyte concentration. The *on* and *off* sets of responses are, hence, based on different charge transport regimes and for this reason independent one of each other resulting in an overall multi-parametric response OTFT operation. This is a unique OTFT sensor characteristic. Recently, evidences were provided that the OTFT response is affected by the contact resistance variation only when operated in the *off*-regime, while the channel conductance is affected in the *on*-regime [31].

Looking at the OTFT sensing mechanism it is crucial to consider that its sensing element is constituted by the organic active layer, where the conduction takes place. This is generally a polycrystalline film usually described as formed by contiguous grains having a crystalline core and amorphous grain boundaries. In fig. 6 a sketch of the energy barrier at the interface between two contiguous organic grains is reported. The polycrystalline nature of the active layer strongly influences both conduction and sensing mechanism of these devices. The charge transport in organic materials is modeled as the result of the contribution of two phenomena: an inter-grain charge transport and the conduction across the grain boundaries. Both being thermally activated transport properties. This is described by the multiple trapping and thermal release (MTR) model, widely used to model transport in a-Si:H TFTs and generally applied to describe polycrystalline OTFTs at room temperature [28]. The organic films have been modeled as systems with a narrow delocalized conduction band and a high concentration of localized lower energy electronic states situated in the gap, which act as low mobility trap states. Such traps can be due to impurities as well as to structural defects located in the crystalline grain and at the grain boundaries [32,33]. During the inter-grain transport, while moving from source to drain through the delocalized levels, the charge carriers of the organic semiconductor interact

with the localized levels. This causes the charges to eventually get trapped. Nevertheless, thanks to the gaining of an activation energy of several tens of meV, carriers can be thermally released. The mobility generally increases with increasing the gate bias since at low gate bias the induced charges are mostly trapped in low mobility states.

As the bias is increased the Fermi level at the insulator/organic interface reaches the closest band edge. At this point the lower energy trap states are all filled, and the induced charges are now freer to move. Charges are transported from a grain to another grain through grain boundaries moving from source to drain. This transport is limited by the strength of the potential barrier between contiguous grains. The mobility across two grains separated by a grain boundary has been described as [33]

$$(4) \quad \frac{1}{\mu} = \frac{1}{\mu_C} + \frac{1}{\mu_{GB}} \quad \text{with} \quad \mu_{GB} \propto \exp\left[-\frac{E_B}{kT}\right] \quad \text{and} \quad E_B = \frac{e^2 n_t^2}{8\epsilon_r \epsilon_0 p},$$

where  $\mu_C$  is the single crystal mobility,  $\mu_{GB}$  is the mobility across the grain boundary,  $E_B$  is the potential barrier between the grains,  $\epsilon_r$  is the dielectric constant of the semiconductor,  $\epsilon_0$  is the permittivity of vacuum,  $n_t$  is the surface density of charged traps at the grain boundaries,  $p$  is the carried density, and  $k$  and  $T$  are the Boltzmann constant and temperature, respectively [32, 33].

Since OTFT  $V_t$  and  $\mu$  depend on the volume density of trapped charges and on the potential barrier between contiguous grains, the conduction mechanism plays a crucial role in determining the sensing mechanism of an OTFT sensor. Indeed, when organic active layers are exposed to several chemical species charge trapping or detrapping processes may occur. As an effect, an increase or a decrease of barriers between the grains can occur.  $V_t$  and  $\mu$  are influenced by the interaction of the transistor active layer with a chemical species and this results in a change of the device on-current. OTFT sensing properties have been proved for different types of active layers such as substituted thiophene-based polymers and oligomers, naphthalenes, copper phthalocyanines, and pentacene. At the same time a wide range of chemical analytes and different analytes, such as alcohols, ketones, thiols, nitriles, esters, and ring compounds have been sensed with these systems [34]. The active layer-analyte interaction has been always modeled as the analyte molecules being adsorbed at the surface of the grains [35]. On the other hand, analyte molecules can also reach the interface with the gate dielectric through the voids between grains [36]. The strength of the interaction with the analyte increases by increasing the grain boundaries exposed to the odor molecule demonstrating the crucial role played by the grain boundaries in the OTFT sensing mechanism [37, 38]. During this process the analyte molecules being trapped at the grains boundaries causes a change of the barrier potential height,  $E_B$ , changing the film mobility according to eq. (4). Beside trapping a minor doping effect has been also observed in specifically designed OTFT sensor/odor systems [36, 38].

**3.1. OTFT selectivity.** – The detection of chemical analytes by means of OTFT sensors is obtained by exploiting the interactions taking place at the analyte molecules/OTFT active layer interface. Organic films implemented in OTFT sensors generally show a quite weak selectivity toward organic molecules such as alcohols or alkenes. On the other hand, it has been demonstrated that it is possible to modulate their specificity by substituting the organic molecules backbones, such as CPs, with properly chosen functional groups [11]. In the presence of the analyte molecules a partitioning of the analyte molecules in the film occurs, similarly to what happens to a stationary phase in a chro-

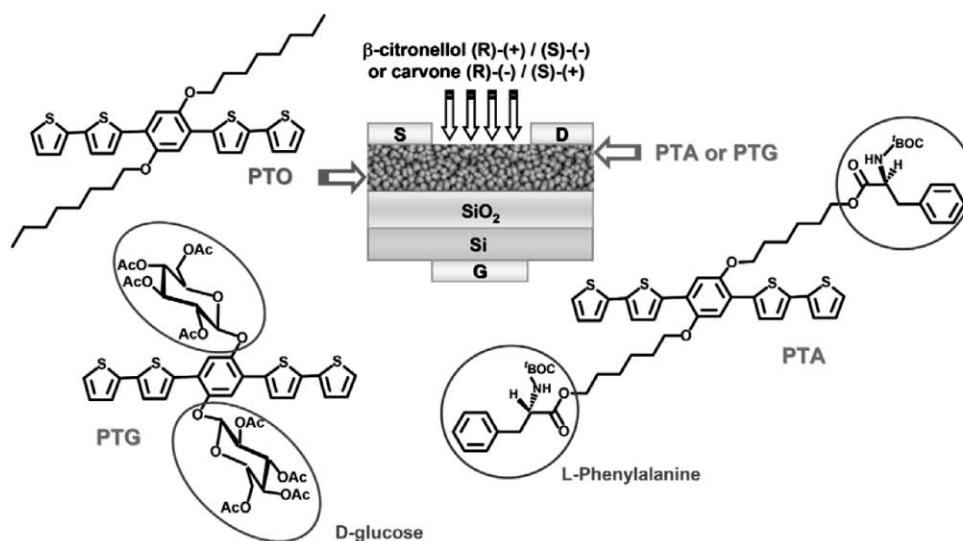


Fig. 7. – Bilayer OTFT chiral sensor structure [3].

matographic column [39]. The OTFT sensing mechanism can be hence described as involving surface-mediated weak interactions between the functionalized organic molecules and the analyte. The adsorption of the odor molecule on the organic film grains appears to be modulated by the degree of chemical affinity between the odor molecule and the functional groups. For this reason, a proper chemical functionalization of the organic material forming the active layer can result in a film that, through the surface of its grains, is able to control the partition coefficient of analytes into the active layer improving OTFT selectivity [35, 40-42].

Hierlemann *et al.* proposed for the first time the interesting approach of using side-chain functional groups to confer broad selectivity to chemical sensors based on a set of polysiloxanes [39]. CPs have been then employed also in a chemiresistor-type configuration to promote the detection of nonpolar vapors [11, 43]. Different linear chains have also been used both as substituents of polythiophene based sensing layers and as analyte molecules to study their influence on the selectivity of CP based sensing devices [35]. Polythiophenes bearing alkyl and alkoxy side groups have been implemented as sensing layers in OTFT and quartz crystal microbalance (QCM) devices to sense different organic vapors such as alcohols, alkanes, and ketones. It has been demonstrated that alkyl and alkoxy side chains, influencing the polar character of the polymers, act as a driving force during the interaction with the analytes. It has been observed that the responses of polar alkoxy substituted polythiophene OTFTs correlate very well when plotted *versus* the analyte dipole moment while no clear trend is observed for the responses of the non-polar active layer, namely an alkyl polythiophene one [35]. On the contrary, good linear correlation can be observed between the responses of the alkyl substituted material and the analyte alkyl chain length. No correlation with the analyte alkyl chain length can be seen for the polar active layer [35].

Remarkable appear some recent results reporting on a new OTFT system for highly selective sensing applications. Figure 7 presents a novel bilayer OTFT structure proposed

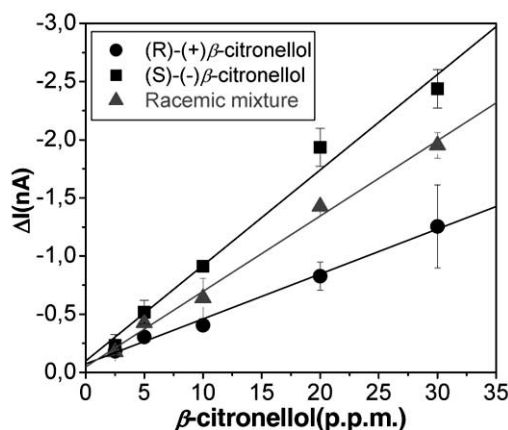


Fig. 8. – Calibration curves of the chiral bilayer OTFTs exposed to (S)-(-)- $\beta$ -citronellol, (R)-(+)- $\beta$ -citronellol [3].

as high performance chiral sensor [3]. These bilayer OTFT sensors have been demonstrated to allow for the chiral differential detection of very low concentration of citronellol and carvone molecules. Two different conjugated oligomers are implemented in this sensing OTFT. A bilayer structure is here used to combine field-effect and chiral recognition properties. As is possible to see in fig. 7, the two layers consist of similar alkoxyphenylene-thiophene oligomers differing just in the side group structure, named PTO, PTA and PTG in the figure. The study here mentioned reports the case of the L-phenylalanine amino acid and the  $\beta$ -O-D-glucosidic substituents. They confer the chiral recognition properties to PTA and PTG, respectively.

The field-induced on-state responses of the PTO-PTA-bilayer OTFT to both the citronellol enantiomers as well as to the racemic mixture of vapours are reported in fig. 8.

Very good calibration curves linearity (with  $R$  better than 0.991), as well as good response repeatability (within 5% RSD) have been reported for this system. The sensitivity differences in the calibration curves for the PTO-PTA OTFT against the two enantiomers are clearly apparent. It is interesting to note as the sensitivity for the racemic mixture (50% of each enantiomer) falls right in between the previous two. This is the first work reporting on OTFT differential discrimination of enantiomers at the part per million level. Moreover this example is particularly relevant, as citronellol enantiomers discrimination is difficult even by common chromatographic techniques. In analogy to this experiment differential recognition of carvone has been obtained by exploiting PTO-PTG bilayer OTFT sensors [3].

Some interesting studies of hole-transporting phenylene-thiophene tetramers, with and without hydroxyl functionalization, interacting with dimethyl methylphosphonate (DMMP), which simulates phosphonate nerve agents, have been also recently published too [44]. 5,5'-bis(4-*n*-hexyl-phenyl)-2,2'-bithiophene (6PTTP6) and 5,5'-bis(4-hydroxyhexyloxyphenyl)-2,2'-bithiophene (HO6OPT) have been here used as active materials in a double-layer OTFT structure whose first layer was constituted by a thin 6PTTP6 film and the second layer was made of a blend of the 6PTTP6 and HO6OPT materials. Hydroxy group of HO6OPT is used as the simplest receptor enhancing this

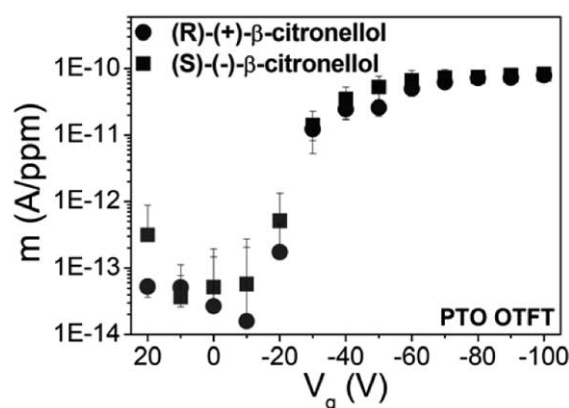


Fig. 9. – Sensitivity enhancement of an OTFT sensor.

interaction while the bilayer structure is here used to exploit the good electrical properties of 6PTTP6, which determines the channel performances of the OTFT, and the sensing properties of HO6OPT. This study shows that the bilayer OTFT responds to DMMP vapour through changes in mobility, threshold voltage, and source-drain current down to 20 ppm concentration [44].

**3.2. Gate-dependent responses.** – One of the main advantages of using a transistor sensor compared to other two terminal devices relies in its capability of modulating the drain current with the gate bias. This property can be advantageous also when an OTFT is used as a sensor. It has been demonstrated, indeed, that OTFT responses depend on the gate bias applied [2, 3, 34-36, 45, 46]. It is well established, in fact, that OTFT responses to fixed concentration of different alcohol vapors increase with increasing the gate bias applied. This effect has been directly correlated to the accumulation mode operation regime of an OTFT. Even though this effect has been widely assessed only very recently the first direct evidence of a gate-field-induced sensitivity enhancement has been given [3]. Figure 9 shows a sensitivity *versus* gate bias plot for an alkoxyphenylene-thiophene OTFT exposed to two citronellol enantiomers [3]. Here the slope values of the calibration curves, along with their associated error bars, are reported as a function of the gate bias applied. As can be noted looking at the figure, a sensitivity enhancement of several orders of magnitude is observable when the device moves from the *off* (gate biases below  $V_t$ ) to the *on* (gate biases above  $V_t$ ) state. The sensitivity values in the plot, namely the slope of the calibration curves taken at different gate bias, are here reported in absolute values. Negative slope values have been recorded for  $V_g > -20$  V (subthreshold regime) while positive slope values have been found for  $V_g < -20$  V.

It has been demonstrated that negative slopes are associated to the channel resistance variation and the positive ones with the contact barrier changes [31]. Contact resistance changes, possibly related to some sort of Schottky barrier, dominate in the subthreshold regime. In other words, they are effective only when the OTFT is in its *off* state. Channel resistance changes, on the other hand, are responsible for the much higher sensitivity taking place in the *on* state [3]. It is interesting to note that the *on* state OTFT responses generally give origin to calibration curves with better linearity properties than *off* state responses. This causes the sensitivity in the *on* state to show lower associated errors than

the sensitivity in the *off* state responses. This could be due to instabilities associated with the subthreshold regime [3].

A similar gate-dependent sensitivity behaviour has been also indirectly observed for an Organic Electrochemical Transistors (OECT) glucose sensor [45]. All these evidences open interesting perspectives for the use of microscopic OTFTs as ultrasensitive electronic transducers that could also operate as sensing switches.

**3.3. Low-voltage operation OTFT sensors for *in liquid testing*.** – One of the main recent challenges of the sensing technology is to develop fast and reliable sensors for on line and *in situ* measurements for in liquid biological applications. Organic transistor sensors are ideal readout devices in this sense. OTFTs offer the great advantage of sensitivity enhancement which can enable very low concentration detection with no need of time-consuming sample preparation. Biological sensing applications take usually place in aqueous media, making low-voltage transistor critical to stable operation in such environment. Electrolytic hydrolysis of water and high ionic conduction through the analyte are, indeed, the principal issues to overcome during in water applications. In this respect traditional OTFTs, which are mainly fabricated on silicon-silicon dioxide substrate, are still high-voltage operation devices with poor in liquid applications unless contact passivation or microfluidic confinement of the sensing area are performed. Beside enabling the operation in aqueous media, low-voltage transistors have attracted great interest particularly for low-power applications. New organic and inorganic dielectrics are currently being developed in order to lower OTFT threshold voltages and inverse sub-threshold slope, both responsible for the high OTFT operation voltages. These figures are mainly regulated by the gate dielectric properties. This makes the research of thin, high capacitance gate dielectrics one of the main challenges of the organic electronic. Remarkable advances in this field have been obtained with the incorporation of ultrathin, cross-linked polymer gate dielectric layers, such as divinyltetramethyldisiloxane-bis(benzocyclobutene) (BCB) [47] or poly(4-vinylphenol) (PVP) cross-linked with trichlorosilanes [48]. Self-assembled monolayer and multilayer dielectrics have also been used to achieve low-voltage operation [49, 50] and low-power complimentary circuits [51]. Alternatively metal oxide based inorganic dielectrics such as  $\text{CeO}_2$ ,  $\text{Y}_2\text{O}_3$ ,  $\text{Al}_2\text{O}_3$ ,  $\text{Ta}_2\text{O}_5$  and  $\text{TiO}_2$  have been also proposed for low-voltage transistors [52-56].

An easy and cheap oxide formation technique has been recently reported [57-59]. This proposes the use of an anodization cell such as the one shown in fig. 10 [4]. During the anodization technique a positive bias is applied to a metal electrode immersed in a weak-acid equipped with a counter-electrode to complete the electric circuit. The electron flow taking place in the circuit drives an electrochemical reaction leading to the formation of an oxide thin film at the anode. The possibility to effectively control the film oxides thickness as well as the easy fabrication procedure in ambient condition and in aqueous media make this approach very appealing. Using this procedure Grell's group has developed a pentacene OTFTs based on anodized  $\text{TiO}_2$  dielectric capped with poly( $\alpha$ -methylstyrene) (PAMS). They have demonstrated exceptional operation below 1 Volt drain and gate voltages, as shown in fig. 11, with carrier mobilities as high as  $0.8 \text{ cm}^2/\text{Vs}$  [4]. Interesting sensing applications of this device can be foreseen.

Roberts *et al.* have recently reported on low-voltage OTFTs capable of stable operation in aqueous media [6]. These OTFTs are based on a thin, cross-linked gate dielectric and a stable organic semiconductor whose structure is depicted in fig. 12. In such a work by Bao's group the gate dielectric is constituted by poly(4-vinylphenol) (PVP) cross-linked with either 4,4'-(hexafluoroisopropylidene)diphtalic (HDA) or suberoyl chlo-

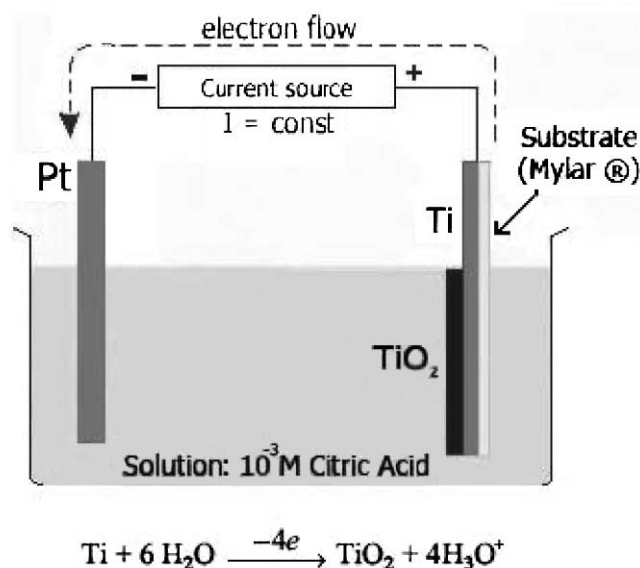


Fig. 10. – Schematic representation of an anodization cell [4].

ride (SC). High capacitance (up to 400 nF/cm<sup>2</sup>) spin coated dielectric cross linked at relatively low temperatures (100 °C) have been obtained allowing for very low voltage operation transistors. OTFT employing different organic active layers have shown very good performances at  $V_d$  and  $V_g$  biases less than 1 V. Exceptional in water operation performances have been demonstrated with 5,5'-bis-(7-dodecyl-9H-fluoren-2-yl)-2,2'-bithiophene (DDFTTF) based cross-linked dielectric OTFT. Long term in water operation has also been proved showing measurements lasting up to 10<sup>4</sup> cycles. DDFTTF OTFTs have been used to detect changes in pH and low concentrations of chemicals. Clear current responses have been recorded allowing for detection of trinitrobenzene up

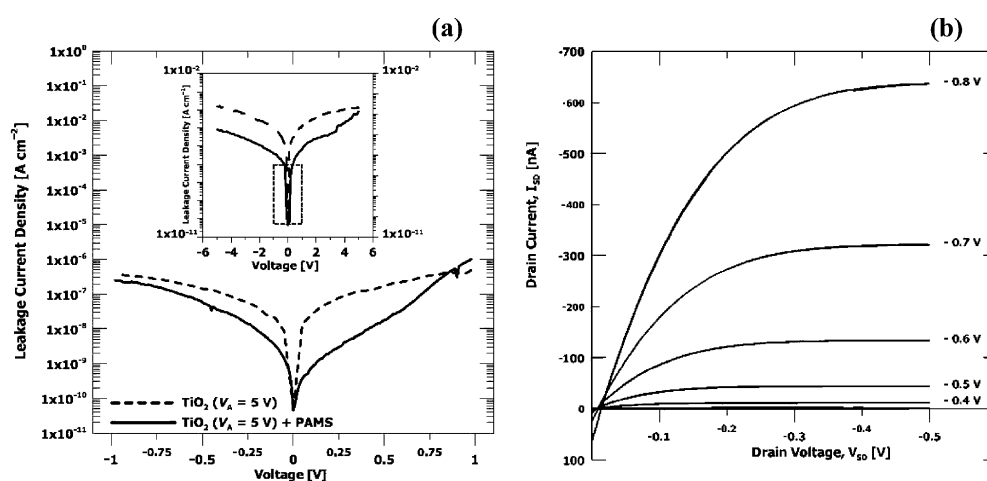


Fig. 11. – Leakage behavior of anodized TiO<sub>2</sub> (a) and output characteristics of pentacene based OTFT with TiO<sub>2</sub> dielectric capped with PAMS (b) [4].

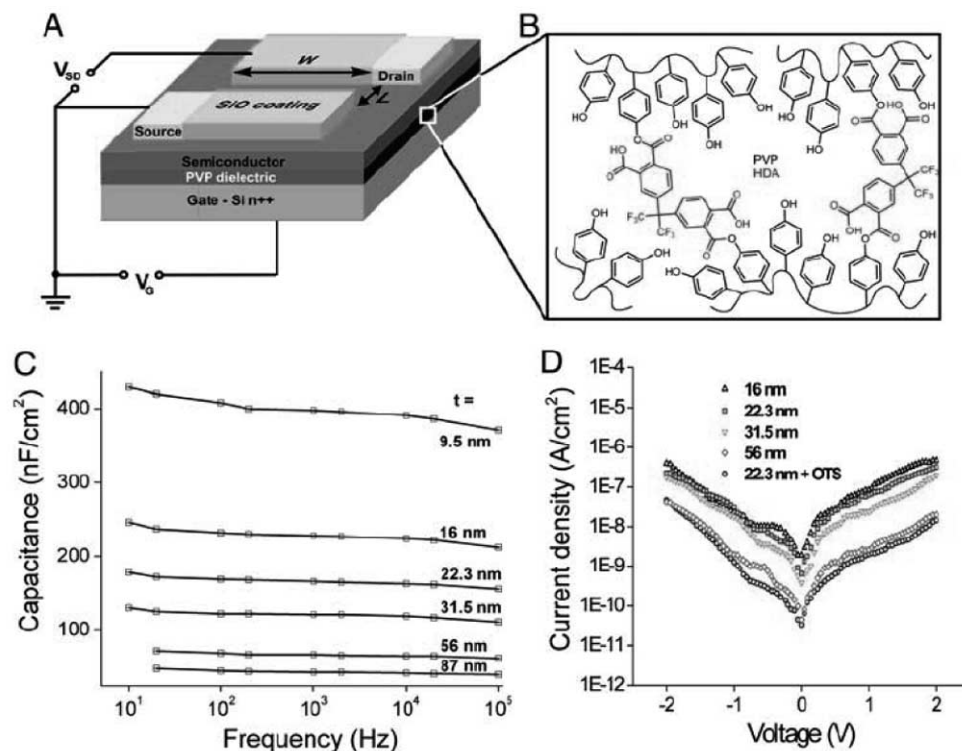


Fig. 12. – Cross-linked polymer gate insulator and its corresponding electrical properties. (A) Structure of the top-contact OTFT sensor. (B) Chemical structure of cross-linked PVP with HDA. (C) Capacitance *vs.* frequency. (D) Leakage current *vs.* voltage for various PVP-HDA films [6].

to 300 ppb, glucose up to 10 ppm, and cysteine up to 100 ppb [6]. The demonstration of robust, high-performance OTFTs that are capable of detecting parts per billion (ppb) analyte concentrations in water open great perspectives in the field of realization of cheap and mass-produced aqueous sensors.

#### 4. – Conclusions

OTFT chemical sensors have demonstrated in the last years to be very promising portable sensors overcoming most of the main drawbacks of presently commercialized sensor technologies. Their implementation in array based sensing systems seems also to be an interesting and feasible application. OTFTs can be indeed operated as multi-parameter sensors with high repeatability. At the same time many evidences have been given on how it is possible to modulate their specificity by properly choosing CP side groups. In this respect many interesting recent advances have been given demonstrating OTFT bio-specificity. Experiments involving enantioselective chiral OTFT sensors [3] as well hydroxy functionalized active layers OTFTs for nerve agents detection have been here reported [44]. Finally this review reports on low-voltage OTFTs for cheap, low-power and mass-produced aqueous sensors [4-6]. Their implementation is recently demonstrated sensors for in liquid biological tests has been discussed.

## REFERENCES

- [1] TORSI L. *et al.*, *Sens. Actuators B*, **67** (2000) 312.
- [2] TORSI L. *et al.*, *Sens. Actuators B*, **93** (2003) 257; TORSI L. and DODABALAPUR A., *Anal. Chem. A*, **77** (2005); WANG L. *et al.*, *Anal. Bioanal. Chem.*, **384** (2006) 310.
- [3] TORSI L. *et al.*, *Nat. Mater.*, **7** (2008) 412.
- [4] LEZEK A. M., RAOUL S. and GRELL M., *Adv. Mater.*, **17** (2005) 192.
- [5] DOST R., DAS A. and GRELL M., *J. Phys. D*, **40** (2007) 3563.
- [6] ROBERTS M. E. *et al.*, *Proc. Natl. Acad. Sci.*, **105** (2008) 12134.
- [7] PERSAUD K. C., *Mater. Today*, **8** (2005) 38.
- [8] WILSON D. M. *et al.*, *IEEE Sens. J.*, **1** (2001) 256.
- [9] JANATA J. and JOSOWICZ M., *Nat. Mater.*, **2** (2003) 19.
- [10] GARDNER J. W. and BARTLETT P. N., *Electronic Noses: Principles and Application* (Oxford Science Publication) 1999.
- [11] BISSELL R. A. *et al.*, *Phys. Chem. Chem. Phys.*, **4** (2002) 3482.
- [12] BERGVELD P., *IEEE Trans. Biomed. Eng.*, BME, **19** (1972) 342.
- [13] LLOYD SPETZ A. and SAVAGE S., in *Recent Major Advances in SiC*, edited by CHOYKE W. J., MATSUNAMI H. and PENSL G. (Springer, Berlin) 2003, pp. 879-906.
- [14] JANATA J. and JOSOWICZ M., *Acc. Chem. Res.*, **31** (1998) 241.
- [15] BERGVELD P., HENDRIKSE J. and OLTUIS W., *Meas. Sci. Technol.*, **9** (1998) 1801.
- [16] BERGVELD P., *Sens. Actuators B*, **88** (2003) 1.
- [17] TORSI L., TANESE M. C., CRONE B., WANG L. and ANANTH DODABALAPUR, in *Organic Transistor Chemical Sensors in Organic Field-Effect Transistors*, edited by BAO Z. (Taylor & Francis Group, New York) 2007.
- [18] NECLIUDOV P. V., SHUR M. S., GRUNDLACH D. J. and JACKSON T. N., *J. Appl. Phys.*, **88** (2000) 6594.
- [19] STREET R. A. and SALLES A., *Appl. Phys. Lett.*, **81** (2002) 2887.
- [20] DIMITRAKOPOULOS C. D. and MALENFANT P. R. L., *Adv. Mater.*, **14** (2002) 99.
- [21] ZIEMELIS K. E. *et al.*, *Phys. Rev. Lett.*, **66** (1991) 2231.
- [22] LANE P. A. *et al.*, *Phys. Rev. Lett.*, **77** (1996) 1544.
- [23] ÖSTERBACKA R. *et al.*, *Science*, **287** (2000) 839.
- [24] HOROWITZ G. *et al.*, *J. Phys. III*, **5** (1995) 355.
- [25] MEIJER E. J. *et al.*, *Appl. Phys. Lett.*, **80** (2002) 3838.
- [26] MEIJER E. J. *et al.*, *J. Appl. Phys.*, **98** (2003) 4831.
- [27] DODABALAPUR A. *et al.*, *Science*, **268** (1995) 270.
- [28] HOROWITZ G., *Adv. Mater.*, **10** (1998) 365.
- [29] MULLER R. S., KAMINS T. I. and CHAN M., *Device Electronics for Integrated Circuits* (John Wiley & Sons, New York) 2003.
- [30] EMIN D., *Adv. Phys.*, **24** (1975) 305.
- [31] TORSI L. *et al.*, *Org. Electron.*, **10** (2008) 233.
- [32] HOROWITZ G. and HAJLAOUI M. E., *Synth. Met.*, **122** (2001) 185.
- [33] POWELL M. J., *Philos. Mag. A*, **43** (1981) 93.
- [34] CRONE B. *et al.*, *Appl. Phys. Lett.*, **78** (2001) 2229.
- [35] TORSI L. *et al.*, *J. Phys. Chem. B*, **107** (2003) 7589.
- [36] TANESE M. C. *et al.*, *Biosens. Bioelectron.*, **21** (2005) 782.
- [37] TORSI L. *et al.*, *J. Phys. Chem. B*, **106** (2002) 12.563.
- [38] WANG L., FINE D. and DODABALAPUR A., *Appl. Phys. Lett.*, **85** (2004) 6386.
- [39] HIERLEMANN A. *et al.*, *Anal. Chem.*, **72** (2000) 3696.
- [40] SOMEYA T. *et al.*, *Langmuir*, **18** (2002) 5299.
- [41] ZHU Z.-T. *et al.*, *Chem. Commun.*, **13** (2004) 1556.
- [42] BARTIC C., CAMPITELLI A. and BORGHES G., *Appl. Phys. Lett.*, **82** (2003) 475.
- [43] GUERNION N. *et al.*, *Synth. Met.*, **128** (2002) 139.
- [44] HUANG J., MIRAGLIOTTA J., BECKNELL A. and KATZ H. E., *J. Am. Chem. Soc.*, **129** (2007) 9366.

- [45] BERNARDS D. A. *et al.*, *J. Mater. Chem.*, **18** (2008) 116.
- [46] SOMEYA T. *et al.*, *Appl. Phys. Lett.*, **81** (2002) 3079.
- [47] CHUA L. L., HO P. K. H., SIRRINGHAUS H. and FRIEND R. H., *Appl. Phys. Lett.*, **84** (2004) 3400.
- [48] YOON M. H., YAN H., FACCHETTI A. and MARKS T. J., *J. Am. Chem. Soc.*, **127** (2005) 10388.
- [49] HALIK M. *et al.*, *Nature*, **431** (2004) 963.
- [50] YOON M. H., FACCHETTI A. and MARKS T. J., *Proc. Natl. Acad. Sci. USA*, **102** (2005) 4678.
- [51] KLAUK H., ZSCHIESCHANG U., PFLAUM J. and HALIKM, *Nature*, **445** (2007) 745.
- [52] INOUE T. *et al.*, *Jpn. J. Appl. Phys.*, **32** (1993) 1765.
- [53] MANCHANDA L. and GURVITCH M., *IEEE Electron Device Lett.*, **9** (1988) 180.
- [54] PANDE K. P., NAIR V. K. R. and GUTIERREZ D., *J. Appl. Phys.*, **54** (1983) 5436.
- [55] ROY P. K. and KIZILYALLI I. C., *Appl. Phys. Lett.*, **72** (1998) 2835.
- [56] KIM H. *et al.*, *Appl. Phys. Lett.*, **69** (1996) 3860.
- [57] TATE J. *et al.*, *Langmuir*, **16** (2000) 6054.
- [58] MAJEVSKI L. A., SCHROEDER R. and GRELL M., *J. Phys. D*, **37** (2004) 21.
- [59] LEZEK A. M., RAOUL S. and GRELL M., *Adv. Funct. Mater.*, **15** (2005) 1017.